Effective Bloch Equations for Semiconductor Lasers and Amplifiers

C. Z. Ning, R. A. Indik, and J. V. Moloney

***Abstract*— A set of effective Bloch equations is established for semiconductor bulk or quantum-well media. The model includes the nonlinear carrier-density dependence of the gain and refractive index and their respective dispersions (frequency dependences). A comparative study is performed between the full microscopic semiconductor Bloch equations and this effective model for pulse propagation to show the range of validity of the present model. The results show that this model agrees well with the microscopic model provided carrier depletion is the dominant saturation mechanism relative to the plasma heating. The effective Bloch equations provide an accurate and practical model for modeling amplifiers with pulses of duration greater than a few picoseconds. By capturing the large bandwidth and the carrier density dependence of the gain, it also provides a reliable model for studying the complex spatiotemporal multilongitudinal and transverse mode dynamics of a variety of wide-aperture high-power semiconductor lasers. The model goes beyond the traditional rate equations and is computationally much more efficient to simulate than the full model.**

***Index Terms*— Gain and index dispersion of semiconductors, many-body effects, nonlinear optical gain, semiconductor amplifiers, semiconductor laser modeling and simulation.**

I. Introduction

THE VERY LARGE gain bandwidth and its nonlinear dependence on carrier density of inverted semiconductor media provides both technological opportunities and fundamental modeling challenges. In a semiconductor amplifier, for example, the carrier density undergoes very large excursions in magnitude as an initially weak injected pulse grows out of a noisy background and the corresponding optical susceptibility function may fluctuate strongly in shape and magnitude. In semiconductor diode lasers, the large gain bandwidth causes the laser to typically run in multiple longitudinal modes unless precautions are taken to suppress the latter by spectral filtering using, e.g., Bragg gratings. Wide-aperture high-brightness laser sources offer even greater challenges leading to multilongitudinal/transverse mode dynamics, dynamic intensity filamentation, and strongly nonuniform carrier density fluctuations both along, and transverse to, the laser structure. One would like to have a robust modeling scheme in which the nonlinear optical response function can adapt on the fly to local density and intensity changes within the structure. The latter optical response could be derived from a first principles microscopic theory or measured experimentally.

In modeling or simulating high-power semiconductor lasers or amplifiers, it is essential to capture those features of the semiconductor (quantum well or bulk) lasers mentioned above: the large gain bandwidth and the large density variations. The phenomenological rate equations used for semiconductor laser modeling, however, do not contain these features. The more complete theory at the microscopic level is computationally too expensive to be used. An alternative beyond these two choices is needed for efficient and accurate modeling. There are some models in the literature [6]–[11] which include gain dispersion. However, we feel that the approach that we will present in this paper is preferable. As we will discuss in detail in the following sections, our approach is derived from the detailed microscopic semiconductor physics and uses more fundamental parameters, like material concentration and quantum-well (QW) structure parameters. In addition, the density as well as the frequency dependence of the susceptibility is built into our model.

This paper is organized as follows. In the second section, we give a detailed account of the background for our approach by reviewing the current approaches based on rate equations and microscopic theory. The calculation of the gain and refractive index from the microscopic theory is then outlined in Section III. This is followed by the approximation of the gain and index and the establishment of our model in Section IV. In Section V, we apply our model to pulse propagation, where we compare the results of the current model with the microscopic theory. In Section VI, we compare the current model with other models that have been proposed [6]–[11]. In the last section, we summarize the main results of this paper and point out possible extension for the future research.

II. Motivation and Background

Rate equations [12]–[14] or their static simplification, the beam propagation model [15], [16] are most widely used for the semiconductor laser modeling. Semiconductor laser performance and the modeling based on these equations have been extensively reviewed elsewhere [15], [16], [14]. The traditional rate equations refer to the set of equations for photon and carrier densities, but here we use this terminology also for the set of equations for complex field amplitude (not intensity or photon density) coupled with carrier density with a linear gain or index change [14]. The advantage of the rate

Manuscript received August 12, 1996; revised February 19, 1997. This work was supported by the Air Force Office of Scientific Research, Air Force Materiel Command, USAF, under Contract AFOSR F 49620-94-1-0144 DEF and Contract AFOSR F49620-94-1-0463 DEF.

C. Z. Ning was with the Arizona Center for Mathematical Sciences, University of Arizona, Tucson, AZ 85721 USA. He is now with the NASA Ames Research Center, Moffett Field, CA 94035-1000 USA.

R. A. Indik and J. V. Moloney are with the Arizona Center for Mathematical Sciences, University of Arizona, Tucson, AZ 85721 USA.

Publisher Item Identifier S 0018-9197(97)06224-6.

equations lies in their conceptual simplicity. In addition, rate equations are very easy to simulate and can capture many of the important features of laser operation.

There are, however, several issues that are especially relevant for broad-area high-power lasers and amplifiers and that are not addressed by simple rate equations. First, as is well known, both gain and index are in general nonlinear functions of carrier density, but the rate equation approach uses linearized gain and index around the transparency or the threshold density. For lasers operating near threshold, this is not a problem since the carrier density is clamped to its threshold value. However, the linear gain/index approximation becomes questionable for broad-area lasers, where there is a significant lateral density change [18]–[21], associated with the complex lateral mode structure [17], and for the monolithical MOPA where longitudinal density changes along the structure are important [24]. Another striking example involving dramatic density change is the formation of the complex transverse mode structures in large aperture vertical-cavity surface-emitting lasers [1]–[3]. In these devices, there is an associated transverse spatial hole burning with significant density variations. In all these structures the carrier density changes are so significant that a linearization of the gain and index around any particular density becomes invalid. In [20], the consequences of this linearization were demonstrated by comparing the linearized gain and the nonlinear gain. It was found that the gain at the lateral edges of the laser (and therefore the beam extent) is overestimated using the linearized gain. In addition inaccurate carrier-induced index profiles lead to poor prediction of lateral beam filamentation.

Second, in the rate equations, a frequency independent gain and index are used, which means that actual gain and refractive index spectra with given curvatures (see Fig. 1) are replaced by frequency independent straight lines. This is a valid approximation for a single-mode laser. For broad-area lasers, MOPA structures, and large aperture surface-emitting lasers, multiple longitudinal modes or complex lateral mode structures appear [1]–[3], [18], [19], [21]. In these cases, each mode sees different gain (and index) depending on their locations in the gain/index spectra. Even small differences in gain for the individual modes will have an important influence on the final laser output. Thus gain discrimination is very critical.

Finally, it has been shown mathematically that the rate equations with diffraction term included are ill-posed, showing very different behavior of instabilities [22] from the full Maxwell–Bloch model with polarization included. The numerical evidence of this ill-posedness is an instability at grid-scale, which might be mistaken for a numerical instability.

The above-mentioned issues are adequately addressed in the full microscopic model [4], [5], known as the Semiconductor Bloch Equations (SBE's), as we will briefly show in Section III. The microscopic theory with many-body interactions included has shown better agreement with experiments [4], [5] for describing optical responses of the semiconductor bulk and QW media than the free-carrier counterpart. The problem with the full microscopic theory in describing spatial-temporal dynamics is the formidable computation involved. The SBE's

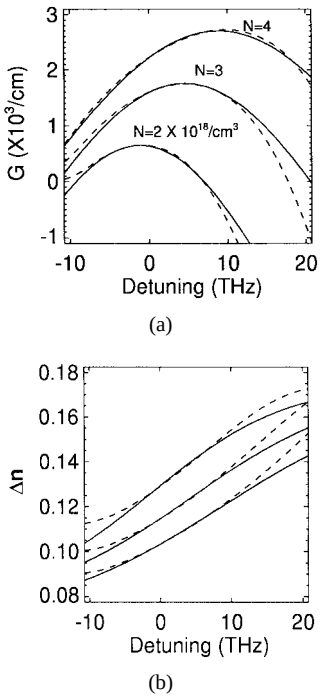

Fig. 1. (a) Gain and (b) carrier-density induced index change for GaAs bulk medium. The detuning is given in $\nu = \omega/2\pi$.[1] The carrier densities are 2×10^{18} cm^{-3}, 3×10^{18} cm^{-3}, and 4×10^{18} cm^{-3}, respectively. The dashed lines are calculated from the microscopic theory directly, while the solid lines are fitted by a single Lorentzian plus the background contribution.

contain, in addition to the intrinsic complexity of the many-body physics involved, time scales from nanoseconds down to 50–100 fs [4]. As a result, numerical simulations using explicit schemes must use very small time steps, while implicit schemes amount to solving very large systems of equations. On the other hand, we require at least a total simulation time well in excess of nanoseconds to study the spatial-temporal dynamics. The electronic wavevector dependence of the polarizations and distribution functions makes the problem one dimension larger than the usual laser equations for a similar geometry.

There is a related issue that makes the computation more expensive for semiconductor lasers. As we mentioned above, the gain bandwidth for semiconductor lasers is typically very large, so that the gain spectrum is quite flat, as we will emphasize later in this paper. This means that the gain discrimination for adjacent modes is very small, leading to the very small difference in the decay or growth rates of neighboring modes. This again requires that the computation time has to be long enough to make a final determination of the long-term dynamical behavior of the lasers, as a result of the neighboring mode competition.

To study the spatial mode structure and lateral filamentation, we need to solve the corresponding partial differential equations at the microscopic level [18], [19]. The addition of the spatial resolution in lateral and/or transverse direction of the laser device, coupled with small time steps and long

[1]It is to be noted that $\Gamma_1 \approx \Delta\omega = 2\pi\Delta\nu$ for a Lorentzian oscillator. Usually $\Delta\nu$ rather than $\Delta\omega$ is used as a measure of the gain bandwidth. A time constant of 5 fs for $1/\Gamma_1$ corresponds to a gain bandwidth of $\Delta\nu = 30$ THz.

computation time, makes the whole problem almost impossible to simulate, even with today's ever increasing computational capability.

From what has been said above, it is clear that a model for semiconductor lasers is needed which satisfies the following criteria. It must adequately address the issues of carrier density dependence and of the dispersion of gain and refractive index and yet remain computationally manageable.

Our approach is the following. For a given QW or bulk epitaxial structure, we calculate the gain and index (susceptibility) spectra using the microscopic theory for a range of carrier densities, typically, from below transparency up to several times the laser threshold. For each density, we parameterize the susceptibility spectrum by approximating the spectrum as a superposition of several Lorentzians. The quantities characterizing the individual Lorentzians then act as our parameters. These parameters are functions of carrier density (and temperature). In this way, the relevant frequency and density dependence are retained. Using these parameterized Lorentzians, we construct a set of equations which satisfy the criteria mentioned above. In the simple case of a single Lorentzian approximation, the set of equations is formally very similar to the Bloch equations for two level atoms, thus we call our model effective Bloch equations (EBE's).

III. Gain and Index Calculation from the Microscopic Theory

Our starting point is the microscopic many-body theory under the Hartree–Fock approximation [4], [5]. For the plasma screening, we use a single plasmon-pole model [5]. The theory leads to the following SBE's [4], [5] for carrier distribution functions $n_{\alpha,k}$ and the envelope polarization variables p_k:

$$\dot{p}_k = -[\gamma_2 + i(\omega_k - \omega_c)]p_k - i\Omega_k \cdot (n_{e,k} + n_{h,k} - 1) \tag{1}$$

$$\dot{n}_{\alpha,k} = \Lambda_{\alpha,k} - \gamma_n n_{\alpha,k} - \gamma_1(n_{\alpha,k} - f_{\alpha,k}) + \frac{i}{4}(\Omega_k * p_k^* - \Omega_k^* p_k), \qquad \alpha = e,h \tag{2}$$

where $\omega_c, \gamma_2, \gamma_1$, and γ_n are the reference frequency, dephasing rate of the polarization, carrier equilibration rate, and carrier loss rate due to spontaneous and nonradiative processes, respectively. The $\Lambda_{\alpha,k}$'s are the pumping rate to individual k state. The ω_k's in (1) and (2) are the renormalized transition frequency for each individual transition at electron wave vector k: $\hbar\omega_k = E_{e,k} + E_{h,k} + E_g + \Delta E_k$, with $E_{e,k}$ and $E_{h,k}$ being the conduction band and valence band single particle energies, respectively, and E_g the bare bandgap. The bandgap shrinkage due to many-body interactions ΔE_k is a density-dependent function [4]. The Ω_k's are the generalized Rabi frequency including the "internal field" due to the Coulomb interactions: $\Omega_k = (\mu_k/\hbar)E + (1/\hbar)\Sigma_{k' \neq k}\ V_{|k-k'|}p_{k'}$. E is the complex laser field envelope and $V_{|k-k'|}$ is the screened Coulomb potential in Fourier representation, $\hbar$ is Planck's constant divided by 2π, and μ_k is the dipole transition elements which are obtained through the bandstructure calculation.

To obtain the linear susceptibility function, (1) and (2) are solved in Fourier domain. Under the Padé approximation [5], the intensity gain (G), the carrier-induced index change (δn), and the susceptibility $(\chi(N,\omega))$ are expressed in the form [4]

$$\chi(N,\omega) \equiv -\frac{i}{K}G(N,\omega) + \frac{2}{n_b}\delta n(N,\omega) = \frac{1}{\epsilon_0\epsilon_b V}\sum_k \frac{|\mu_k|^2(f_{e,k} + f_{h,k} - 1)}{\gamma_2\hbar + i\hbar(\omega_k - \omega_c - \omega)}Q_k \tag{3}$$

where we assume that carriers obey Fermi–Dirac statistics with distribution functions $f_{e,k}$ and $f_{h,k}$ characterized by a total density $N = (1/V)\Sigma_k\ f_{e,k} = (1/V)\Sigma_k\ f_{h,k}$ and plasma temperature T_p. As a result, the gain and index depend only on total density, frequency ω, and plasma temperature. In (3) Q_k is the so-called Coulomb enhancement factor [4], [5]. $K = \omega_c n_b/c$ is the optical wavevector in the medium of background index n_b, with c being the speed of light in the vacuum. Other parameters in (3) are defined as follows: ϵ_0 and $\epsilon_b = n_b^2$ are the dielectric constant in the vacuum and the relative dielectric constant of the medium, respectively. Many-body effects manifest themselves in two ways in the above expression. The individual transition frequency (denoted by ω_k above) is "renormalized" by the Coulomb interaction [4], [5] and the dipole transitions are modified by the Coulomb enhancement factor Q_k (see [4] and [5]).

Our consideration is quite general and is applicable to both QW structures and bulk medium. The index k in the summation of (3) contains spin index and in the case of the QW structure, also the confined band indices, in which case, the k should be understood as the wavevector in the plane of the QW layer. In the case of the QW, we must first calculate the confined bands and the bandstructure for all the confined valence bands.

The first step to construct our model is to parameterize the gain and index as calculated using the microscopic theory. To begin with, we fix the plasma temperature T_p as a constant in the present model. The susceptibility is therefore a function of two variables: density N and frequency ω. Generally, we require that the susceptibility $\chi(N,\omega)$ calculated through (3) for a given laser structure be approximated by superposition of several Lorentzians, namely,

$$\chi(N,\omega) \approx \chi_0(N) + \sum_l^M \frac{A_l(N)}{i\Gamma_l(N) + (\delta_0 + \omega - \delta_l(N))} \equiv \chi_0(N) + \sum_l^M \chi_l(\omega, N) \tag{4}$$

where $\chi(N,\omega)$ is given by (3), and we also include a "background" contribution $\chi_0(N)$ which is frequency independent. In (4), we use a detuning parameter: $\delta_0 = \omega_c - E_g/\hbar$. Note that we allow the density dependence of the "parameters" $A_l(N), \Gamma_l(N)$, and $\delta_l(N)$ for the individual Lorentzian oscillators. In general, we expect to approximate the susceptibility function quite well using only a few such oscillators. Therefore, this approach could be called a few-oscillator approximation for the semiconductor gain medium. It is important to point out that for many applications it suffices to have only one such Lorentzian oscillator plus the "background" absorption and index. An example for this

approximation is shown in Fig. 1 where gain and index spectra for bulk GaAs, calculated from the microscopic theory for three different densities, are plotted (solid lines) together with the spectra of the approximations using (4) (dashed lines). The physical meaning of this one oscillator is very simple: $A_1(N)$ essentially determines the strength of the Lorentzian. $\Gamma_1(N)$ determines the bandwidth of the spectrum which changes with density. $\delta_1(N)$ represents the gain peak shift with the density, as is obvious from Fig. 1. We see that using one oscillator we basically capture all of the essential features of the gain/index spectra. Our next step is to establish a set of equations using this approximated susceptibility $\chi(N,\omega)$ as given by (4).

IV. The Effective Bloch Equations (EBE's)

Though most of the calculations in this paper are concerned with the case of one oscillator, we will construct our model for the general case of multiple oscillators. One reason is that, at the higher excitation of the QW medium, the transitions involving the second subband can be important, so that a gain spectrum with two peaks may appear. In this case, a single oscillator will definitely not be enough to approximate the gain spectrum.

To construct our model equations, we note that, by obtaining the gain and refractive index spectra for a given semiconductor structure in the last section, we have actually solved the p_k equations (1). This fact together with our parameterization means that we have the following relation:

$$\frac{1}{V}\sum_k \mu_k p_k = P_0 + P_1 + P_2 + \cdots \tag{5}$$

where $P_0, P_1, \cdots$ are the polarizations corresponding to the individual Lorentzians, which we obtain by constructing their Fourier components $\tilde{P}_j(\omega)$ through the relation

$$\begin{aligned}\tilde{P}_0 &= \epsilon_0\epsilon_b\chi_0(N)\tilde{E}(\omega),\\ \tilde{P}_j(\omega) &= \epsilon_0\epsilon_b\tilde{\chi}_j(N,\omega)\tilde{E}(\omega)\\ &= \frac{\epsilon_0\epsilon_b A_j(N)\tilde{E}(\omega)}{i\Gamma_j(N)+\delta_0+\omega-\delta_j(N)}, \qquad j=1,2\cdots\end{aligned} \tag{6}$$

where quantities with a $\tilde{}$ represent their Fourier transforms. If we perform the inverse Fourier transform of (6), we obtain

$$\begin{aligned}\frac{dP_j(t)}{dt} &= \{-\Gamma_j(N)+i[\delta_0-\delta_j(N)]\}P_j(t)\\ &\quad -i\epsilon_0\epsilon_b A_j(N)E(t), \qquad j=1,2,\cdots\end{aligned} \tag{7}$$

while for $(j=0)$ we have $P_0(N)=\epsilon_0\epsilon_b\chi_0(N)E(t)$, because no frequency dependence of $\chi_0(N)$ is assumed. It is important to note that, in performing the Fourier transformation, we have treated density-dependent functions $\Gamma_j(N), \delta_j(N), A_j(N)$, and $\chi_0(N)$ as if they were independent of time. In fact this is not the case, because these functions depend on a time-varying density. However, this is still a good approximation as long as carrier density changes much more slowly compared to the inverse gain bandwidth. This is obviously true in a typical laser. For very strong and short pulses, this may not be a good assumption.

Next we derive an equation for the total carrier density. This is achieved by summing the k-resolved density equations (2) using (5). This leads to

$$\begin{aligned}\frac{dN}{dt}-\frac{\partial}{\partial x}D_N\frac{\partial N}{\partial x} &= -\gamma_n N+\frac{\eta J}{ew}+\frac{i}{4\hbar}\\ &\quad\cdot[(P_0+P_1+\cdots)^*E\\ &\quad -(P_0+P_1+\cdots)E^*]\end{aligned} \tag{8}$$

where we have added the carrier diffusion term with diffusion constant D_N in the lateral direction (x). The parameters η, J, e, w are respectively, the quantum efficiency, pumping current, electron charge, and active region thickness. In deriving (8), we have used the following relations:

$$\frac{1}{V}\sum\Lambda_{\alpha,k}=\frac{\eta J}{ew} \tag{9}$$

$$\sum_k\sum_{k'}V_{|k-k'|}p_k^*p_{k'}=\sum_k\sum_{k'}V_{|k'-k|}p_kp_{k'}^*. \tag{10}$$

The corresponding equation for the laser field amplitude is written as

$$\frac{\partial E}{\partial z}-\frac{i}{2K}\frac{\partial^2 E}{\partial x^2}+\frac{n_g}{c}\frac{\partial E}{\partial t}=\frac{iK\Gamma}{2\epsilon_0\epsilon_b}(P_0+P_1+\cdots) \tag{11}$$

where n_g is the group index and we also introduce the confinement factor Γ in (11).

Equations (7), (8), and (11) form the basic set of equations for our model. These equations contain density-dependent parameters which must be obtained from the independent calculation of gain and index spectra, or from experimental measurements.

For a given laser system, our first step is to parameterize the susceptibility function using (4). The simplest way of satisfying (4) is to do a best fit of the actually calculated $\chi(\omega,N)$ for a given density using the right-hand side of (4) as a fitting function. Such fittings for a range of densities offer density dependence of the functions $A_j(N), \Gamma_j(N), \delta_j(N)$, and $\chi_0(N)$. In Fig. 2, we show the density dependences of these functions. One remarkable thing to note is that the width of the Lorentzian, which corresponds directly to the gain bandwidth[2] in the case of single oscillator approximation, is quite large. The corresponding time constant changes approximately from 5 to 3 fs[3] for densities between $1\times10^{24}/\mathrm{m}^3$ and $5\times10^{24}/\mathrm{m}^3$, which is ten to twenty times smaller than the individual polarization decay time. We will discuss this further when comparing with other models in Section VI.

To deal with those density-dependent functions ("parameters") that appear in (7), (8), and (11), we note that the density dependence of these parameters could be well approximated by linear functions of density within a certain density range, as can be seen from Fig. 2. This allows us to have an explicit set of equations which is useful when doing certain analyses. In numerical simulation, however, it is rather straightforward to use rational function fits for these functions. Equations (7), (8), and (11) with parameters given as rational functions of density can then be quite efficiently solved. Equations (7), (8), and (11), for the case of single oscillator without the lateral

[2] See footnote 1.

[3] See footnote 1.

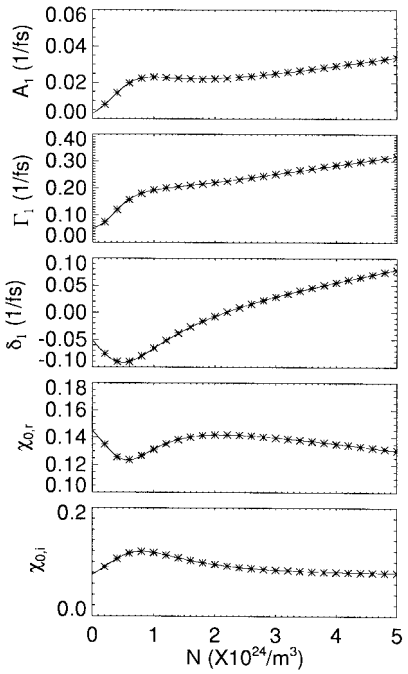

Fig. 2. Plotted are "parameters" of the Lorentzian oscillator and the real $(\chi_{0,r})$ and imaginary $(\chi_{0,i})$ parts of the "background" susceptibility. Stars are calculated using the microscopic theory, while solid lines are fits to the rational functions that are used in numerically solving the EBE's.

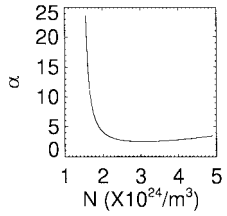

Fig. 3. Linewidth enhancement factor (α) obtained using the fitted susceptibility function at a fixed frequency 30 meV below the bare bandgap of the GaAs.

derivatives, are similar in form to the standard Maxwell–Bloch equations for the two-level system. The essential difference lies in the density dependence of the parameters plotted in Fig. 2.

To conclude the presentation of our model, we point out that, since we now have an expression for the susceptibility expressed as function of density-dependent parameters, many important quantities such as differential gain and the linewidth enhancement factor [28], [29] (α) can be written explicitly. Especially in the case of the single Lorentzian, the linewidth enhancement factor can be expressed in a rather simple form. Fig. 3 shows an example of α at a fixed frequency near gain peak as a function of carrier density using our parameterized χ. This value is consistent with the α values given in [4]. This should, of course, be expected, since the parameterized χ is a good approximation of that computed microscopically.

V. Application to Picosecond Pulse Propagation

Picosecond pulse propagation in a semiconductor amplifier provides a stringent test of the EBE model, both because the energy of the pulse will grow quite large so that carrier density varies significantly, and because plasma heating may become important. The application of the present model to the broad-area lasers and MOPA will be presented elsewhere [23]. In this section, we consider pulse propagation in a bulk GaAs amplifier. The parameters we use are standard ones for GaAs. The corresponding microscopic theory was presented in Section III. Pulse propagation using the full microscopic theory has been extensively studied elsewhere [30]–[32].

For the electric field amplitude, we solve the propagation equation for the laterally plane wave with a transverse confinement factor of 0.2 for a bulk medium. The medium is modeled by (1) and (2). Scattering processes are approximated by time constants of 80, 170, and 300 fs for carrier–carrier, and electron–phonon, and hole–phonon scatterings, respectively. The plasma temperature is extracted from the actual distribution function obtained. Fig. 4 shows a comparison of propagations of a Sech-shaped pulse using the full model [(1), (2), (11)] and the EBE's [(7), (8), and (11)] with an initial pulse FWHM of 20 ps. Fig. 4(a) shows two sets of almost indistinguishable pulse profiles, with the slightly lower profile representing the propagation of the full microscopic model. The medium is initially inverted at a carrier density of 3×10^{18} cm^{-3}. The initial pulse amplitude is 6 meV which corresponds to roughly the saturation intensity [30]–[32] for this pulsewidth. As we can see, the pulse is not significantly amplified, but mostly reshaped. We observe good agreement for reshaping of the two profiles, despite the plasma temperature profile plotted in Fig. 4(b) with a temperature rise above lattice temperature (300 K) of about 10 K. We also compare an initially very weak pulse of similar width. The agreement is consistently as good as shown in Fig. 4. To see when the present model will fail, we reduce the width of the pulse to 2 ps. We start from an initial amplitude as weak as 0.1 meV. Fig. 5(a) shows the final stage of the pulse propagation. At the earlier stage the agreement is very good. We see, however, that the two profiles start to diverge as the pulse propagates, with the peak amplitude of the EBE model growing faster. In Fig. 5(b), we see the plasma temperature increases up to around 20 K over the lattice temperature. This plasma temperature rise is responsible for the earlier saturation of pulse predicted by the full model.

In general, what we see are the two competing effects that lead to pulse saturation. The first one is the familiar one due to carrier depletion, determined by the pulse energy, roughly given by peak intensity times the pulsewidth. The second one is due to plasma heating. Which of the two appears first with the propagation depends on the initial pulse intensity and width, and the particular medium properties. In our present EBE model, the effect of plasma heating is not included. Only the first saturation mechanism can appear. In the first case (Fig. 4), the pulse energy reaches a saturation value before plasma temperature rises too high. The saturation of peak intensity then halts the plasma heating. In the second case (Fig. 5) the opposite happens. Before the pulse energy reaches the saturation value, the plasma temperature is already significantly elevated above lattice temperature and gain is depleted. The pulse begins reshaping as predicted by the full model, while the EBE model shows a further amplification

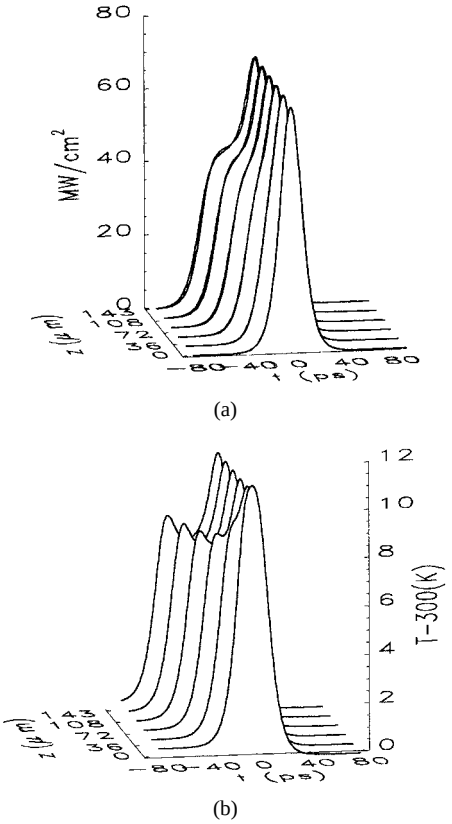

Fig. 4. Pulse propagation in a bulk inverted medium. (a) Pulse intensity profiles and (b) the corresponding plasma temperature elevation. The two pulse profiles are almost indistinguishable, with the slightly lower one representing the results of the full model.

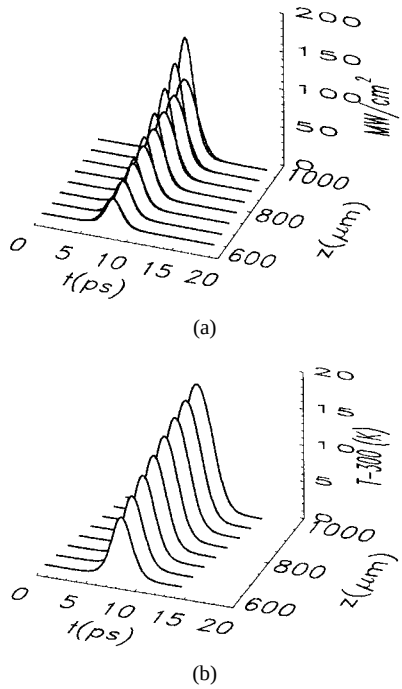

Fig. 5. Same as Fig. 4, but for a shorter pulse of 2 ps. The thick line in (a) shows the result of the EBE model. The initial pulse intensity is very weak, but only the later stage of propagation is shown in the figure.

due to the absence of the plasma heating mechanism. From our experience, we can conclude that the two models agree well for a plasma temperature rise roughly within 10 K. In a typical laser, the time scale involved should be larger than a picosecond, and the peak intensity is much lower. Therefore, the EBE model should be a useful model for the broad-area lasers and MOPA's.

It is to be emphasized that the computation time is drastically reduced in the EBE model compared to the full SBE's. In the EBE model, only a few variables need to be calculated at each spatial point. However, at first glance, it may appear that the wide gain bandwidth, as reflected by the large value of $\Gamma_1(N)$, will still require very small time steps. This can be avoided by using a semi-implicit scheme based on the one used in [33]. This method would not be practical for the SBE system, since the large (200 by 200, say) linear systems would have to be solved at each step for each spatial point. Using this scheme in the EBE model, the step size is not limited by the Γ_1, but by the dynamics of the electrical field. In our simulation of the above pulse propagations, the SBE system typically requires CPU time 1000 times those required by the EBE's.

VI. Comparison to the Other Models

We are aware of a few other models proposed recently [6]–[11] to describe semiconductor lasers and amplifiers with inclusion of gain and/or index dispersions. These models can be divided into two categories: those adding dispersion terms [6]–[8] to the field equations and those including a polarization equation [9]–[11]. With the exception of [10], the density dependence of gain and refractive index dispersions is not included in these models. The basic idea of [6]–[8] is to expand the linear gain and refractive index in the frequency domain up to second order. The frequency-dependent gain is Fourier transformed to time domain, leading to an equation for the field amplitude containing the second-order time derivative. Of course, such a Taylor expansion of the susceptibility in Fourier space can be applied to our expression for χ as given in (4), so the coefficients in the equations in [6]–[8], can be derived from the values of the parameters that we calculate. However, the derived values of those coefficients will be density dependent. This dependence was not treated in their models. This was not a problem for simulations of pulse propagation where the pulse energies were low enough so that the density did not vary a great deal. For high energy pulses, or for simulation of high power lasers, the density variation can be quite large. The comparison in [7] and [8] to experiments is very impressive and shows that for subpicosecond pulses it is necessary to include the effects of plasma heating. This is included in their model via a linear dependence of gain on temperature, with the temperature driven by free-carrier absorption, stimulated emission, and two-photon absorption. In addition, the gain and refractive index spectra in their models are expanded in Taylor series up to second order. This is very often a good approximation for many practical applications, but to capture asymmetrical gain spectra, higher order expansion is necessary. This leads to higher order time derivatives. This should be compared with the necessity to include more Lorentzian oscillators (thus more polarization

variables) in our approach. In both cases, the order of the system is increased. However, the Taylor expansion approach is less suited to dealing with the QW medium at higher densities. In that case, the higher QW subbands are involved, so that the gain spectrum can show two peaks. Of course, any arbitrary smooth shape can be approximated with a sufficient number of terms, but high-order time derivatives will lead to systems of equations that are numerically more intractable. The approximation using multiple Lorentzians is more natural in this setting and is numerically less difficult.

In another development, two-level-like Bloch equations were used for modeling semiconductor lasers [9]–[11]. In deriving these models, the authors of [9] and [11] used an approximation that led to a single polarization equation with a relaxation rate of the individual k-resolved polarization. This is equivalent to the homogeneous-broadening limit in gas lasers. Unfortunately, this is a poor approximation for semiconductor medium which is in the domain of the inhomogeneous limit with a very large inhomogeneous linewidth (the gain bandwidth), as can be seen in Fig. 1. As we see from Fig. 2, the values of the Γ_1 curve change from the 5×10^{13} s^{-1} to around 30×10^{13} s^{-1}. This is the typical gain bandwidth[4] of a semiconductor medium, consistent with experimental measurements [34]. In [9], [11], as well as in [6], however, the homogeneous linewidth of individual oscillators of 1×10^{13} s^{-1} was used as the gain bandwidth, or equivalently as the effective polarization decay constant. As a consequence of this underestimated gain bandwidth, pulse broadening in time domain could be overestimated in [6]. One could use values for the linewidth in the models of [6], [9], and [11] that would lead to values for gain bandwidth that are more realistic, but without a density dependence, one could not use these models to calculate behavior of systems where the density has a large variation. We note that in a somewhat different approach [10] a relaxation constant corresponding to a realistic gain bandwidth was obtained for the free-carrier case. The density dependence of gain spectrum was also considered there. However, it seems difficult to include many-body interactions using their approach.

VII. Conclusion

In summary, we have constructed a model for semiconductor lasers and amplifiers. The main motivation is to bridge the gap between two well-established theories: the rate equations on the one hand and the microscopic many-body theory on the other. The two issues, density and frequency dependence of the gain and refractive index that are contained in the microscopic many-body theory, are addressed now at the macroscopic level by a parameterization procedure. Our model is tested in the case of pulse amplification. The main application of the present model is to describe the broad-area lasers and amplifiers with transverse and/or longitudinal extension. The usefulness of the model to these problems will further be demonstrated in a forthcoming publication [24]. One of the advantages of the present model is that the resultant equations, the EBE's, can now be solved much more efficiently. At the same time, the EBE's are formally very similar to the Bloch equations of the two-level atoms. This makes the equations more easily accessible by researchers without detailed knowledge of many-body theory. Finally we want to emphasize that the procedure can be equally well applied to experimentally measured gain and index spectra.

Perhaps the most important extension of this work now underway is the inclusion of the effects of plasma heating. We have seen that the EBE's do an excellent job of modeling pulse propagation in semiconductor media provided the plasma heating is not a strong factor in gain saturation (see Figs. 3 and 4). As was mentioned in the derivation of the EBE's, we can take into account not only the effects of density dependence of the susceptibility, but also the effects of the plasma heating. In order to include this effect in a self-consistent fashion, it is necessary to sum the $n_k \hbar^2 k^2/(2m)$ to obtain an equation for the kinetic energy, in much the same way that n_k was summed to produce (8) (cf. [24]–[27]). In this way, the present method can be extended to describe the propagation of shorter and higher energy pulses.

[4] See footnote 1.

References

[1] K. Tai and Y. Lai, "Transverse mode emission characteristics of gain-guided surface emitting lasers," *Appl. Phys. Lett.*, vol. 63, pp. 2624–2626 1993.

[2] H. Li, T. L. Lucas, J. G. McInerney, and R. A. Morgan, "Transverse modes and patterns of electrically pumped vertical-cavity surface-emitting lasers," *Chaos, Solitons, and Fractals*, vol. 4, pp. 1619–1636, 1994.

[3] F. B. De Colstoun, G. Khitrova, A. Fedorov, T. Nelson, C. Lowry, T. Brennan, and B. Hammons, "Transverse modes, vortices and vertical-cavity surface-emitting lasers," *Chaos, Solitons, and Fractals*, vol. 4, pp. 1575–1596, 1994.

[4] W. W. Chow, S. W. Koch, and M. Sargent, *Semiconductor Laser Physics*. Berlin, Germany: Springer-Verlag, 1994.

[5] H. Haug and S. W. Koch, *Quantum Theory of the Optical and Electronic Properties of Semiconductors*, 2nd. Singapore: World Scientific, 1993.

[6] G. P. Agrawal, "Effect of gain dispersion on ultrashort pulse amplification in semiconductor laser amplifiers," *IEEE J. Quantum Electron.*, vol. 27, pp. 1843–1849, 1991.

[7] M. Y. Hong, Y. H. Chang, A. Dienes, J. P. Heritage, and P. J. Delfyett, "Subpicosecond pulse amplification in semiconductor laser amplifiers: Theory and experiment," *IEEE J. Quantum Electron.*, vol. 30, pp. 1122–1131, 1994.

[8] A. Dienes, J. P. Heritage, C. Jasti, and M. Y. Hong, "Femtosecond optical pulse amplification in saturated media," *J. Opt. Soc. Amer. B*, vol. 13, pp. 725–734, 1996.

[9] C. Bowden and G. P. Agrawal, "Maxwell–Bloch formulation for semiconductors: Effects of coherent Coulomb exchange," *Phys. Rev. A*, vol. 51, pp. 4132–4139, 1995.

[10] J. Yao, G. P. Agrawal, P. Gallion, and C. Bowden, *Opt. Commun.*, vol. 119, pp. 246–255, 1995.

[11] S. Balle, "Effective two-level-model with asymmetric gain for laser diodes," *Opt. Commun.*, vol. 119, pp. 227–235, 1995.

[12] H. Statz and G. A. de Mars, in *Quantum Electronics*, C. H. Towns, Ed. New York: Columbia, 1960, pp. 503–537.

[13] H. Haken, "Light," in *Laser Light Dynamics*. Amsterdam, The Netherlands: North-Holland, 1985, vol. 2.

[14] G. P. Agrawal and N. K. Dutta, *Long-Wavelength Semiconductor Lasers*. New York: Van Nostrand-Reinhold, 1986.

[15] G. Hadley, J. Hohimer, and A. Owyoung, "Comprehensive modeling of diode arrays and broad-area devices with applications to lateral index tailoring," *IEEE J. Quantum Electron.*, vol. 4, pp. 2138–2152, 1988.

[16] J. Buus, "Principles of semiconductor laser modeling," *Proc. Inst. Elect. Eng.*, vol. 132, pt. J, pp. 42–51, 1985.

[17] R. J. Lang, A. G. Larsson, and J. G. Cody, "Lateral modes of broad-area semiconductor lasers: Theory and experiment," *IEEE J. Quantum Electron.*, vol. 27, pp. 312–320, 1991.

[18] O. Hess, "Spatial-temporal complexity in multi-stripe and broad-area semiconductor lasers," *Chaos, Solitons, and Fractals*, vol. 4, pp.

1597–1618, 1994.
[19] O. Hess, S. W. Koch, and J. V. Moloney, "Filamentation and beam propagation in broad-area semiconductor lasers," *IEEE J. Quantum Electron.*, vol. 31, pp. 35–43, 1995.
[20] P. Ru, J. V. Moloney, R. Indik, S. W. Koch, and W. W. Chow, "Microscopic modeling of bulk and quantum-well GaAs-based semiconductor lasers," *Opt. Quantum Electron.*, vol. 25, pp. 675–693, 1993.
[21] H. Adachihara, O. Hess, E. Abraham, P. Ru, and J. V. Moloney, "Spatiotemporal chaos in broad-area semiconductor lasers," *J. Opt. Soc. Amer. B*, vol. 10, pp. 658–665, 1993.
[22] P. K. Jakobson, J. V. Moloney, A. C. Newell, and R. Indik, "Space-time dynamics of wide-section lasers," *Phys. Rev. A*, vol. 45, pp. 8129–8137, 1992.
[23] J. V. Moloney, R. A. Indik, and C. Z. Ning, "Full space-time simulation for high brightness semiconductor lasers," *IEEE Photon. Technol. Lett.*, vol. 9, pp. 731–733, 1997..
[24] T. L. Koch, L. C. Chiu, C. Harder, and A. Yariv, "Picosecond carrier dynamics and laser action in optically pumped buried heterostructure lasers," *Appl. Phys. Lett.*, vol. 41, pp. 6–8, 1982.
[25] B. N. Gomatam and A. P. DeFonzo, "Theory of hot carrier effects on nonlinear gain in GaAs-GaAlAs lasers and amplifiers," *IEEE J. Quantum Electron.*, vol. 26, pp. 1689–1704, 1990.
[26] A. Uskov, J. Mork, and J. Mark, "Wave mixing in semiconductor laser amplifiers due to carrier heating and spectral-hole burning," *IEEE J. Quantum Electron.*, vol. 30, pp. 1769–1781, 1994.
[27] C. Z. Ning, R. A. Indik, and J. V. Moloney, "Self-consistent approach to thermal effects in vertical-cavity surface-emitting lasers," *J. Opt. Soc. Amer. B*, vol. 12, pp. 1993–2004, 1995.
[28] H. Haug and H. Haken, "Theory of noise in semiconductor laser emission," *Z. Phys.* vol. 204, pp. 262–275, 1967.
[29] C. H. Henry, "Theory of the linewidth of semiconductor lasers," *IEEE J. Quantum Electron.*, vol. QE-18, pp. 259–264, 1982.
[30] A. Knorr, R. Binder, M. Lindberg and S. W. Koch, "Theoretical study of resonant ultrashort-pulse propagation in semiconductors," *Phys. Rev. A*, vol. 46, pp. 7179–7186, 1992.
[31] R. A. Indik, J. V. Moloney, R. Binder, W. W. Chow, A. Knorr, and S.W. Koch, "Many-body effects in the propagation of short pulses in a semiconductor amplifier," in *SPIE Proc.*, 1995, vol. 2399, pp. 650–659.
[32] R. A. Indik, R. Binder, M. Mlejnek, J. V. Moloney, S. Hughes, A. Knorr, and S. W. Koch, "Role of plasma cooling, heating, and memory effects in subpicosecond pulse propagation in semiconductor amplifiers," *Phys. Rev. A*, vol. 53, pp. 3614–3620, 1996.
[33] J. A. Fleck, "Ultrashort-pulse generation by Q-switched lasers," *Phys. Rev. B*, vol. 1, pp. 84–100, 1970.
[34] D. J. Bossert and D. Gallant, "Gain, refractive index, and α-parameter in InGaAs-GaAs SQW broad-area lasers," *IEEE Photon. Technol. Lett.*, vol. 8, pp. 322–324, 1996.

C. Z. Ning received the B.S. and M.S. degrees in physics from the Northwestern University, Xi'an, China, and the Ph.D. degree in physics from the Institute from the University of Stuttgart, Germany, in 1991, under Hermann Haken. His dissertation concerned nonlinear dynamics of lasers and other optical systems.

As part of his dissertation research at the Institute for Theoretical Physics, University of Stuttgart, he discovered the geometric phase in self-pulsing lasers, making the first connection between the geometric phase and phase space attractors in dissipative dynamical systems. After receiving the Ph.D. degree, he continued his research there with the SFB project, Molecular Electronics, until 1994, when he joined the Arizona Center of Mathematical Sciences, University of Arizona, Tucson, initially as a Post-Doctoral Research Associate and later as a Research Assistant Professor. Recently, he joined NASA Ames Research Center as a Senior Research Scientist. He was a Visiting Scientist at the University of Stuttgart in 1986 and a Lecturer at Northwestern University, China, in 1987–1988. His past research areas also included nonlinear dynamics, stochastic resonances, plasma heating, and other thermal effects in semiconductor lasers. Currently, his research interest includes optical and electronic properties of semiconductor quantum structures, comprehensive and self-consistent modeling and simulation of semiconductor optical and electronic devices, and spatio-temporal dynamics of broad-area semiconductor lasers and amplifiers.

R. A. Indik, photograph and biography not available at the time of publication.

J. V. Moloney, photograph and biography not available at the time of publication.